BULLETIN OF THE POLISH ACADEMY OF SCIENCES
TECHNICAL SCIENCES, Vol. 73(5), 2025, Article number: e154285
DOI: 10.24425/bpasts.2025.154285

An innovative pendulum-based absorber exploiting time-varying mass dynamics for vibration damping

Bogumil CHILINSKI[1], **Rafal KWIATKOWSKI**[2], **Krzysztof TWARDOCH**[1], and **Anna MACKOJC**[1]*

[1] Institute of Machine Design Fundamentals, Warsaw University of Technology, Poland,
[2] University of Kalisz, Poland

Abstract. Research concerns an innovative semi-active pendulum absorber utilising a varying mass as a way of controlling mechanical system dynamics. An objective of the study is to propose the attenuator concept and its mathematical model – an attachable device mounted to a vibrating system in order to eliminate its pendulum motion. The main advantage of the novel pendulum tuned mass damper (PTMD) is combining features of widely known vibrational energy absorber (TMD), improving and expanding its capability through allowing for adaptable changes to the system characteristics and extending its basic operational range through varying its mass realised by transferring the fluid between the main system and the absorber. The article provides research comparing the results of computer simulations with empirical experiments. The objective was to investigate the effectiveness of mass transfer in process of vibrations mitigating. Various factors were analysed, including the influence of changes in a natural frequency of the structure, the activation time of a tuned mass damper (TMD), and the fluid flow rate within the system. The findings demonstrate that mass transfer is a promising approach to reduce vibrations in both, mechanical systems and civil engineering structures. Presented approach enhances the performance of conventional TMDs by incorporating variable parameters, leading to more effective vibration damping compared to traditional fixed-parameter designs.

Keywords: tuned mass damper (TMD); semi-active damper; variable mass; system dynamics control; sweeps frequency response; pendulum motion control.

1. INTRODUCTION

When considering design and operation of machinery, equipment, buildings or other architectural structures, the phenomenon of mechanical vibration is often classified as an undesirable motion, which in unfavourable conditions can lead to a reduction of durability occurring in reduced service life and malfunctions such as noise or reduced quality of operation, resulting in damage of the structure. The discussed phenomenon is commonly analysed taking into account the three aspects [1], which are:

- Impact on machine quality (faster machine wear out);
- Machine failure rate (vibroacoustic diagnostics);
- Quality of work and health of operators (vibroacoustic protection).

Designers are keen to follow the trend to design engineering structures with a higher durability simultaneously caring for an improvement of their users' comfort. For this purpose, various types of vibration eliminators are installed on structures or are formed as their part.

The current research on vibration suppression can be divided into three main control methods used in dynamic structures:

- Passive control systems – technically simple devices or structural elements, built such that the system as a whole is able to dissipate energy provided by the excitation independently to the external energy sources [2,3]. An important part of passive eliminators are so-called dynamic vibration absorbers. They modify the natural frequency of a structure giving contribution to a reduction of effects of dynamic loads. Moreover, they are characterised by stability of their parameters, which cannot be intentionally modified during the operation [4].
- Active control systems – utilise external actuators responsible for introducing additional forces counteracting to the system dynamic loads. Active vibration eliminators are automatically adjustable systems mounted on the structure and their main elements are sensors, a computer and actuators triggering an appropriate control force [4].
- Semi-active control systems – they combine properties of both, passive and active, vibration dampers. Similarly to the active systems, they are built of sensors, computer and actuators, but they do not require such a high power supply to reduce vibrations [5–10].

An interesting example of vibration attenuation systems is a tuned mass damper. A device consists of a comparatively light mass (in comparison to a whole structure) mounted on springs and is used in structures to reduce mechanical vibrations. Its working principle is based on a simple rule – to tune its vibration frequency near the resonant frequency of the object it is mounted to. The operational principle of a TMD relies on adjusting its natural frequency to coincide with a specific dynamic response of the host structure – most commonly, its resonant frequency. This frequency tuning enables the redistribution of vibrational energy, thereby reducing the peak amplitude of the

*e-mail: anna.mackojc@pw.edu.pl

Manuscript submitted 2025-01-07, revised 2025-04-23, initially accepted for publication 2025-05-05, published in July 2025.

structural response by shifting the effective dominant frequency away from that of the external excitation. It is important to note that TMDs are not constrained to resonance mitigation alone; they can be precisely tuned to target and suppress vibrations at any prescribed frequency component introduced by external dynamic loading, thus offering a versatile solution for vibration attenuation across a wide spectrum of excitation conditions.

An important feature of TMDs is that no additional energy is required - making the solution passive vibration absorber. TMDs are most often used in automobiles and buildings [11–15]. Besides being very popular, the most important feature of TMDs is their lossless operation. The "damping" phenomenon happens by a pure change of the system characteristics without energy dissipation. The main disadvantage is a narrow operational range. In recent years, a new group of damping solutions have become more popular. The papers [16] and [17] present an adaptive tuned mass damper (ATMD) with the ability to adjust its stiffness or damping ratio adaptively to current situation. This is realised by introducing an active element (an actuator) into a basic TMD, which based on a control strategy can overcome the shortcomings of passive solutions. However, these often require high energy supply. A large-scale study on semi-active TMDs, conducted by Chinese researchers, explored various approaches to vibration control. Their research focused on how modifying the physical properties of structures or integrating AI-based methods can enhance vibration suppression. Various studies have explored advancements in tuned mass damper (TMD) systems for vibration control. [18] and [19] introduce PTMD with geometric nonlinear dampers for seismic response control. [20] examined pedestrian-induced vibrations with human-structure interaction, and [21] developed an adaptive-passive MTMD with automatic mass adjustment for improved performance. Lastly, [22] and [23] proposed a semi-active TMD with variable damping and stiffness, outperforming conventional designs in reducing displacements and base forces. It should be noted that vibration damping in engineering solutions is mostly based on a use of semi-active control methods. The method commonly used for vibration control is an application of magnetorheological (MR) fluids. Several reviews of MR fluid applications, in-depth analyses of their models and control strategies can be encountered in recent years [24–26]. The higher effectiveness in vibration control might be obtained when changing parameters of the system during its operation with a utilisation of adjustable damping. However, such an approach causes energy loss resulting from its dissipation. It constitutes a disadvantage of such solutions as the energy is irretrievably lost and converted into heat. In studies [27, 28] and [29] one can find conclusions regarding modelling, analysis and testing of a particle impact damper. The device is composed of a container filled with a granular material and characterised by a passive damping ability resulting from grain-grain and grain-container collisions that however might be adjusted based on changes in the device parameters. Another interesting approach to vibration attenuation based on changes to the system parameters is presented in [30]. Among solutions of adjustable damping, special attention should be paid to research presented in [31]. The authors analyse dynamics of a double pendulum system for a varying mass as a parameter. The study covers three cases where the mass change occurs in the upper, lower and in both members of the pendulum system. The investigation contains the analysis of the influence of this phenomenon on the considered system behaviour. It was concluded that the system is sensitive to change of the system mass, which causes it to behave in a desired manner. A constant and variable mass system of a double pendulum is presented in a similar approach in [32]. The mathematical and physical model confirms throughout the research that the variable mass phenomenon can be used as a factor enabling suppression of the system vibrations in practical application. Moreover, the basic articles [33] and [34] presenting and explaining the mass exchange phenomenon as a way of vibration attenuation are previous studies of one of the authors.

2. RESEARCH OBJECTIVES

A few of these analyses allow us to notice shortcomings and gaps to improve the system operation using common features of well-known solutions. For this reason, the authors decided to propose a concept of vibration absorber utilising a variable mass allowing for its use as a part of the absorber structure design. Most of the studies regarding potential utilisation of the system variable mass to damp vibrations encountered in literature were mostly experimental research. What is more, a negligible number of such products available on the market is the evidence of not much success in the discussed field. One can find hardly any information regarding the implementation of such a device. All of the aforementioned factors induce a need for a proposal of a novel device combining features of other solutions. The authors decided to rely on the working principle of a passive TMD system simultaneously improving and expanding its capabilities through adding an ability to turn it on or off when it is needed or desired allowing for adaptable changes to the system characteristics extending its operational range. The systems operating with changeable parameters perform more effectively contrary to systems of constant parameters (TMDs). The authors proposed a solution based on a pendulum system in order to absorb or control the system oscillations. An addition of an extra pendulum member to the main pendulum system corresponds to the concept of the TMD system, however its operation range is extended by an influence on its dynamics resulting from a property of a variable mass. The mass variability is realised through the use of fluid overflow within and between the pendulums. A liquid is used as an absorber and throttling its flow allows a semi-active control [35–37]. The encountered studies support the concept of effective fluid utilisation. The additional contributor of the proposed solution, not found in other research, is use of a coupling principle. This fact gives an opportunity to propose a novel solution combining a semi-active control strategy consisting of time variable parameters, as well as very effective (narrow ranges) mass dampers. The main objective of the research conducted is to develop a concept of an innovative vibration absorber using the phenomenon of mass change in the system under consideration. Such system, designed and tested under experimental conditions could be successfully implemented as an alternative and extremely effective solution for

limiting undesirable vibrations of engineering structures. These types of systems could be widely used in the industry, however their particular application is seen in maritime industry, where the utilisation of fluids seems to be natural, for example tanks, oil rigs, etc.

3. PENDULUM ABSORBER DESIGN AND MODELLING

3.1. Pendulum absorber design

Modelling methods and assumptions presented in the paper are necessary to study the proposed concept in order to provide basic limitations and requirements for the process of the absorber design as an initial step for further investigation of the presented solution. A double pendulum with a varying mass was adopted as a model of the considered system. The subject of research is a dynamic system consisting of two connected elements. These elements are stiff enough to be considered as rigid bodies. This approach enables to avoid minor problems with internal vibrations of the structure related to its continuous properties. Accordingly to the principle of mass conservation, it is assumed that the mass of the system as a whole is constant. Additionally, the mass of water flows inside the system from the upper to the lower part of the pendulum according to the arbitrary selected time-history of changes (it can be obtained with a flow control system in the form of sensor and proportional valve). Authors decided to utilise the flow rate characteristics, which fulfils conditions of three operation ranges:

- First range describes the initial state, where the entire amount of fluid is stored in the main member (absorber off).
- Second stage is a liquid transfer between upper and lower elements.
- And the last stage, when fluid is contained in the absorber (lower pendulum).

It allows the entire structure to be treated as a constant-coefficients model in the first and third stage of operation. It is worth noting, this manuscript does not focus on control, which would require a separate device and dedicated study. Instead, the focus here is on the absorber effect on vibrations in a system with varying mass. The classification into stages helps to describe the absorber performance rather than suggesting active regulation of the system dynamics. A test stand was designed primarily as a reference to verify the model, rather than to fully validate the phenomenon across all presented scenarios. The methodology follows a structured approach, beginning with preliminary numerical research to examine the influence of damping and activation time on system amplitude attenuation in the presence of transferred liquid for the considered mathematical model. To validate the developed model, a test stand was constructed, and experimental tests were performed. Upon obtaining results that aligned with the numerical model, the authors proceeded with further research, including numerical simulations on transferred liquid mass influence in the main system, and PTMD and performed sweep frequency analysis. The aforementioned goals and assumptions lead to a nontrivial, novel problem, which seems to be an interesting approach to common engineering problems occurring in fields of slender structures containing fluid, where the system total mass is dominated by the stored medium. Due to the surroundings, i.e., the marine environment, the key industry, in which the application of a semi-active vibration absorber seems to be natural is the offshore industry. The multitude of problems regarding the stabilisation of offshore structures caused by environmental conditions (sea state, wind gusts) abounds in many possibilities of using the proposed approach for the attenuation of a system vibration. The application of the device utilising the phenomenon of mass change as a semi-active side tilt compensator of the ship, floating drilling platforms or floating wind turbines can contribute to increasing safety, improving operational efficiency and reduce operating costs by improving their stability. This makes the technology attractive to the offshore industry in particular [38–42]. By manipulating the mass distribution on board, it is possible to generate torques to counteract the vessel swing motion. The use of this technology could allow the stabilisation system to dynamically adapt to changing sea conditions, which would increase safety during operations or navigation. In addition, the control of mass distribution could lead to the optimisation of fuel operating efficiency by reducing hydrodynamic drag and reducing energy consumption, which is important for the economic operation of the vessel. With this approach, the vessel will be able to maintain better stability even in difficult weather conditions. By reducing undesired movements of floating offshore turbines or drilling platforms, such as tilting or rolling, the quality of operations can be improved, which is crucial in the case of precision drilling operations. Additionally, optimising the stabilisation of offshore platforms and turbines can bring economic benefits through reducing energy and fuel consumption. Lower load on engines and drive systems can lead to reduced operating costs and reduced air pollution. The practical implementation of the double pendulum with a variable mass is made of two hollow rods connected to each other. Additionally, they are connected by the elastic pipe conveying the liquid that gravitationally flows from the upper to the lower member.

3.2. Pendulum absorber modelling

In this study, a mathematical double pendulum presented in Fig. 1 was adopted as a model at the first stage being a simplification of the model aimed – the physical double pendulum.

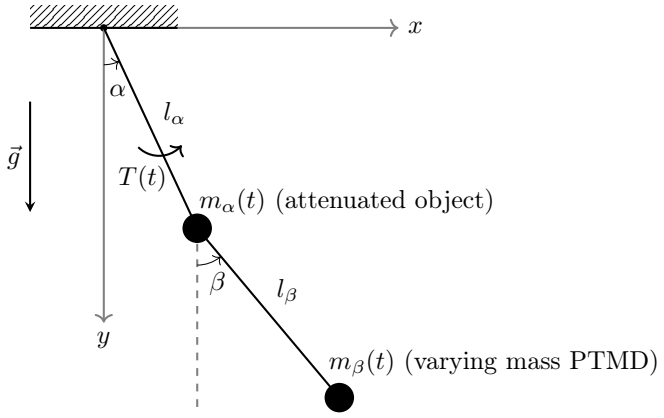

Fig. 1. Scheme of a mathematical double pendulum – a simplified model adopted in the analysis

The dynamics of a double pendulum is complex and can exhibit both regular and chaotic behaviour, depending on initial conditions, system parameters and external excitation. In the regime of small oscillations, where the angles of displacement are relatively small, the motion of a double pendulum can be more predictable and will not involve full rotations. Under these conditions, the system behaviour can be approximated by linearising the equations of motion, leading to solutions that resemble those of simple harmonic oscillators. Therefore, while the mathematical model of a double pendulum can approximate the behaviour of a physical double pendulum in certain low-energy, small-angle scenarios, this approximation breaks down in more energetic or large-angle situations where the full nonlinear dynamics must be considered. However taking into account the mentioned purpose of the system, amplitudes of oscillations are to be limited at some controlled point so the large-angle displacements will not occur. Therefore, while the system operates under low-energy conditions, the mathematical double pendulum closely mimics the physical one, making it an effective approximation for many practical applications. Authors based their choice of the model on a previously conducted research [43, 44]. The mathematical description and analysis was based on classical formalism of Lagrange's equations of a second kind, which was used for a system of two degrees of freedom with smooth, holonomic constraints, using the force of gravity as a potential force. The change in mass has been modelled by the phenomenon of gravitational outflow of liquid from a tank with a hole. It was assumed that the movement of the tank does not disturb the outflow. Lagrange mechanics is used in order to determine the equations of motion for the considered system [45–47]. For this purpose, a Lagrange function must be determined. Lagrangian describes a dynamic state of the system unequivocally. The Lagrange function L is equal to a difference between the kinetic (T) and potential (V) energy of the system:

$$L = T - V. \tag{1}$$

To determine the total energy of the system, the kinetic and potential energies of the individual members are determined. The sum of the individual components represents the kinetic and potential properties of the whole structure. In the case under consideration, the total energy of the system is equal to the sum of kinetic and potential energy of the upper and the lower pendulum member. The final relationship is obtained by inserting the energies into the Lagrange function. The resulting equation forms the basis for further dynamic calculations and allows the equations of motion to be determined. Finally, the kinetic potential (the Lagrange function after substitution) has the following form (2):

$$\begin{aligned} L = {} & \frac{\left(l_\alpha \sin(\alpha)\dot{\alpha} + l_\beta \sin(\beta)\dot{\beta}\right)^2 m_\beta}{2} \\ & + \frac{\left(-l_\alpha \cos(\alpha)\dot{\alpha} - l_\beta \cos(\beta)\dot{\beta}\right)^2 m_\beta}{2} + \frac{l_\alpha^2 m_\alpha \dot{\alpha}^2}{2} \\ & - g\left(-l_\alpha \cos(\alpha) - l_\beta \cos(\beta)\right) m_\beta \\ & - g l_\alpha \left(1 - \cos(\alpha)\right) m_\alpha, \end{aligned} \tag{2}$$

where

t – time;
$\dot{\alpha}$ – angular (generalised) velocity of the upper pendulum member;
g – acceleration of gravity;
α – angle of the upper pendulum swing;
l_α – length of the upper pendulum;
l_β – length of the lower pendulum;
m_α – initial mass of the upper pendulum member;
β – angle of the lower pendulum swing;
m_β – initial mass of the lower pendulum member;
$\dot{\beta}$ – angular (generalised) velocity of the lower pendulum member.

The dissipative potential for the considered system is expressed as follows:

$$D = \frac{b\dot{\alpha}^2}{2} + \frac{b\dot{\beta}^2}{2}. \tag{3}$$

The individual components of the equations of motion are determined by calculating the appropriate derivatives. After calculating the derivatives, the results are inserted into the Lagrange equations. Finally (after substitution), the following system of equations of motion is obtained. The governing equations of the system have a following form (4)–(5):

$$\begin{aligned} & b\dot{\alpha} + \dot{m}_\alpha(t) l_\alpha^2 \dot{\alpha} + \dot{m}_\beta(t) l_\alpha^2 \dot{\alpha} + l_\alpha^2 m_\alpha(t)\ddot{\alpha} + l_\alpha^2 m_\beta(t)\ddot{\alpha} \\ & \quad + g l_\alpha m_\alpha(t) \sin(\alpha) + g l_\alpha m_\beta(t) \sin(\alpha) \\ & \quad + \dot{m}_\beta(t) l_\alpha l_\beta \cos(\alpha - \beta)\dot{\beta} + l_\alpha l_\beta m_\beta(t) \sin(\alpha - \beta)\dot{\beta}^2 \\ & \quad + l_\alpha l_\beta m_\beta(t) \cos(\alpha - \beta)\ddot{\beta} = T_0 \sin(\Omega t), \end{aligned} \tag{4}$$

$$\begin{aligned} & b\dot{\beta} + \dot{m}_\beta(t) l_\beta^2 \dot{\beta} + l_\beta^2 m_\beta(t)\ddot{\beta} + g l_\beta m_\beta(t) \sin(\beta) \\ & \quad + \dot{m}_\beta(t) l_\alpha l_\beta \cos(\alpha - \beta)\dot{\alpha} + l_\alpha l_\beta m_\beta(t) \cos(\alpha - \beta)\ddot{\alpha} \\ & \quad - l_\alpha l_\beta m_\beta(t) \sin(\alpha - \beta)\dot{\alpha}^2 = 0, \end{aligned} \tag{5}$$

where

k – spring stiffness;
Ω – excitation frequency;
$\ddot{\beta}$ – angular (generalised) acceleration of the lower pendulum member;
u_0 – initial difference of spring length and starting spring length;
$\dot{m}_\alpha$ – mass of the upper pendulum and fl and fluid flow;
$\ddot{\alpha}$ – angular (generalised) acceleration of the upper pendulum member;
b – damping coefficient value;
$\dot{m}_\beta$ – mass of the lower pendulum and fluid flow.

The excitation was assumed in the form of an external torque, which aligns naturally with the rotational dynamics of the system. This approach allows the excitation to be introduced directly and intuitively within the system setup. The positive direction of the applied torque is defined to coincide with the direction of positive angular displacement. As a result of this formulation, the system load is obtained in the form of a generalised force:

$$T = T_0 \sin(\Omega t). \tag{6}$$

The mass transfer was modelled by the phenomenon of gravitational outflow of the liquid from the tank (upper pendulum member) to the lower member through the conveying elastic pipe. To simplify the modelling process, a flow function was arbitrarily adopted that corresponds to the physical conditions of the process. An atan function was used, which has an almost constant value outside the surroundings of the t_0 value, while for the activation time it ensures a smooth transition between the states. It is assumed that the movement of the pendulum members does not affect the phenomenon of the mass flow. Taking into account the presented assumptions, the mass of the upper pendulum member can be described by the equation:

$$m_{\alpha 0} = \frac{m_0}{2} - \frac{m_0 \operatorname{atan}(\lambda t - \lambda t_0)}{\pi}, \tag{7}$$

where

t_0 – activation time;
λ – fluid flow rate;
m_0 – transferred damping mass.

A series of simulations of the parameter changes were performed for different values and time ranges with application of the mass transfer function. The results are summarised in a table and repesentative values are selected. The activation time and the λ coefficient are crucial for the studied run. Time-histories of fluid flow described by the the formula (7) for obtained values of parameter t_0 and λ are presented in Figs. 2 and 3.

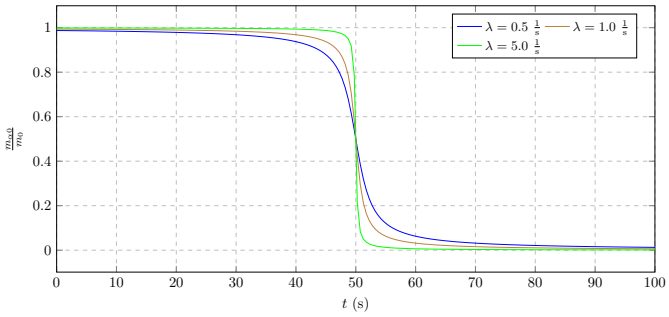

Fig. 2. Flow coefficient changes

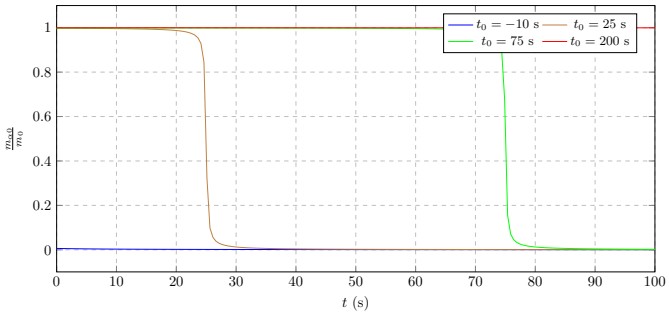

Fig. 3. Opening time changes

The mass of the lower pendulum member was determined on a similar basis to the first pendulum, assuming the same conditions. In addition, it was assumed that the mass of the overflowing fluid is constant. This makes possible to determine the relationship for the mass of the fluid of the lower pendulum member (absorber) in the form of the following formula:

$$m_{\beta 0} = \frac{m_0}{2} + \frac{m_0 \operatorname{atan}(\lambda t - \lambda t_0)}{\pi}. \tag{8}$$

A linearised model of the system can be useful as an initial step of the analysis, as it enables finding a simplified solution in the neighbourhood of the critical point. It is important to distinguish between the process of linearisation and the assumption of constant coefficients. Linearisation refers to approximating the system behaviour around an equilibrium point by neglecting higher-order nonlinear terms, while assuming constant mass simplifies the equations by removing time-dependent variations.

In the simplified calculations, the mass of both members was assumed to be constant. While this introduces some error, the linearised solutions still exhibit qualitative compatibility at the beginning and end of the process (where the fluid mass flow is almost zero). The simplified Lagrangian formulation, incorporating the constant mass approximation, is presented in equation (9):

$$\begin{aligned} L = {} & \frac{l_\alpha^2 m_\alpha(t)\dot{\alpha}^2}{2} + \frac{l_\alpha^2 m_\beta(t)\dot{\alpha}^2}{2} + \frac{l_\beta^2 m_\beta(t)\dot{\beta}^2}{2} + l_\alpha l_\beta m_\beta(t)\dot{\alpha}\dot{\beta} \\ & - \frac{g l_\alpha m_\alpha(t)\alpha^2}{2} - \frac{g l_\alpha m_\beta(t)\alpha^2}{2} - \frac{g l_\beta m_\beta(t)\beta^2}{2} + g l_\alpha m_\beta(t) \\ & + g l_\beta m_\beta(t). \end{aligned} \tag{9}$$

The linearlised equations of motion were derived for the nonlinear model – Lagrangian derivatives were calculated and then substituted into the Lagrange equations. The simplified equations of motion are given the equations (10)–(11):

$$\begin{aligned} & b\dot{\alpha} + l_\alpha^2 \left(\dot{m}_\alpha(t) + \dot{m}_\beta(t)\right)\dot{\alpha} + l_\alpha^2 \left(m_\alpha(t) + m_\beta(t)\right)\ddot{\alpha} \\ & - l_\alpha \left(-g m_\alpha(t) - g m_\beta(t)\right)\alpha + \dot{m}_\beta(t) l_\alpha l_\beta \dot{\beta} + l_\alpha l_\beta m_\beta(t)\ddot{\beta} \\ & = T_0 \sin(\Omega t), \end{aligned} \tag{10}$$

$$\begin{aligned} & b\dot{\beta} + \dot{m}_\beta(t) l_\beta^2 \dot{\beta} + l_\beta^2 m_\beta(t)\ddot{\beta} + \dot{m}_\beta(t) l_\alpha l_\beta \dot{\alpha} + g l_\beta m_\beta(t)\beta \\ & + l_\alpha l_\beta m_\beta(t)\ddot{\alpha} = 0. \end{aligned} \tag{11}$$

Based on the obtained equations of motion, the inertia and stiffness matrices were calculated. The system mass matrix provides a complete description of the behaviour of the system components under the action of accelerations on the individual degrees of freedom. It describes the influence of inertia of the system elements. The mass matrix is given in the following form (12):

$$\mathrm{M} = \begin{bmatrix} l_\alpha^2 \left(m_\alpha + m_\beta\right) & l_\alpha l_\beta m_\beta \\ l_\alpha l_\beta m_\beta & l_\beta^2 m_\beta \end{bmatrix}. \tag{12}$$

The stiffness matrix describes the global response of the system to external forces. The individual components of the matrix result from the elastic and geometrical properties of the overall structure. The stiffness matrix makes it possible to determine the equilibrium positions of the system and, together with the

inertia matrix, to determine its natural frequencies. The stiffness matrix of the system is described as follows:

$$\mathrm{K} = \begin{bmatrix} l_\alpha \left(g m_\alpha + g m_\beta\right) & 0 \\ 0 & g l_\beta m_\beta \end{bmatrix}. \tag{13}$$

The damping matrix represents the total dissipative properties of the system. The individual elements (components) of the matrix result from the damping and geometric properties of the overall structure. The dissipation matrix does not significantly affect the frequency structure of the system (only small shifts of the eigenfrequencies are observed). On the other hand, it has a strong influence on the values of amplitudes. The C matrix is given as follows:

$$\mathrm{C} = \begin{bmatrix} b + l_\alpha^2 \left(\dot{m}_\alpha + \dot{m}_\beta\right) & l_\alpha l_\beta \dot{m}_\beta \\ l_\alpha l_\beta \dot{m}_\beta & b + l_\beta^2 \dot{m}_\beta \end{bmatrix}. \tag{14}$$

A response of the system to an external harmonic force was derived also in analytical form. The amplitude of the attenuated object can be obtained directly from the particular solution. It consists of a numerator that depends mainly on the absorber parameters and a denominator that is equal in value to the determinant of the fundamental matrix. The condition for the tuning of the eliminator can be determined from the fundamental matrix. The analysis of the obtained steady-state solutions makes possible to identify critical points at which the system amplitudes reach unsafe values.

In order to describe the basic properties of the system, its inertia and stiffness matrices will serve to determine an influence of the system parameters on its natural vibration frequencies. The system inertia matrix provides a complete description of the system component behaviour under the action of accelerations on individual degrees of freedom. It describes an influence of inertia of the system elements while the stiffness matrix describes the global response of the system to external forces. The individual components of the matrix result from elastic and geometrical properties of the whole structure. By calculating a determinant of the fundamental matrix, the system natural frequencies can be determined (15), (16):

$$\omega_{n_1} = \frac{1}{2 l_\beta} \left(l_\alpha + l_\beta\right) \sqrt{1 - \sqrt{-\frac{4 l_\alpha l_\beta m_\beta}{\left(l_\alpha + l_\beta\right)^2 \left(m_\alpha + m_\beta\right)} + 1}}, \tag{15}$$

$$\omega_{n_2} = \frac{1}{2 l_\beta} \left(l_\alpha + l_\beta\right) \sqrt{\sqrt{-\frac{4 l_\alpha l_\beta m_\beta}{\left(l_\alpha + l_\beta\right)^2 \left(m_\alpha + m_\beta\right)} + 1} + 1}. \tag{16}$$

Analysing the natural frequency components, some dependencies can be noticed. An expression of "a base frequency" (ω_n^2) can be separated. Its value is being changed by some $\Delta\omega^2$ value. It can be presented as follows:

$$\omega_{n_1}^2 = \bar{\omega}_n^2 \pm \Delta\omega^2. \tag{17}$$

This allows for a more transparent notation of the system natural frequencies. Therefore an easier physical analysis and tuning the system TMD parameters can be done in a more comprehensive and controllable manner.

4. PRELIMINARY EXPERIMANTAL RESEARCH

4.1. Test stand

One of the most effective forms of a verification of theoretical study is to conduct experimental research. Following this principle, the authors decided to build a test stand validating dynamic parameters of the system. In order to validate the correctness of the results, experimental tests were carried out for one exemplary mass configuration and some different values of excitation frequencies. The tests were performed for two frequencies of excitation and the angular acceleration of the main pendulum member $\ddot{\alpha}(t)$ was validated against the results of numerically simulated model. In order to give a satisfactory confirmation of numerical simulation results, the authors decided to design a physical double pendulum model. In parallel with theoretical investigations utilising advanced numerical methods, the decision was made to create a tangible system for experimental verification of vibration damping. The built experimental stand is depicted in Fig. 4. The structure depicted consists of two aluminum profiles, each 500 mm in length, connected to each other by a joint.

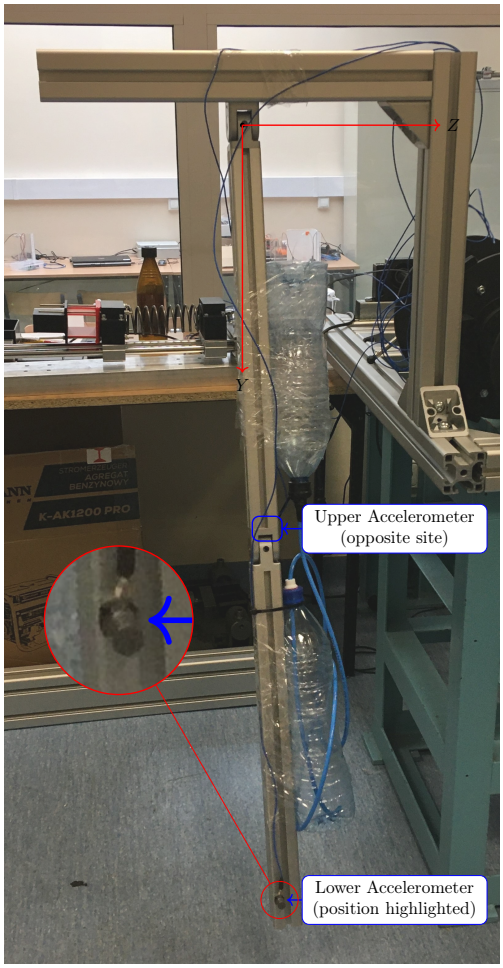

Fig. 4. Test stand

The system is connected to a fixed profile by an articulated joint, allowing precise movements. Liquid tanks are attached to both pendulum members and are connected to each other by a flexible pipe enabling the flow of mass under gravity, from the upper to the lower member of the pendulum. The experimental procedure involved carefully measured the angular acceleration of the pendulum using high-precision sensors. These sensors were calibrated before the tests to ensure the accuracy of the recorded data. For each test, the excitation frequency was controlled by an electric motor, which was coupled to the system allowing precise variation of the frequency and amplitude. Data acquisition was conducted using a digital acquisition system, which recorded the angular acceleration in real-time. The angular acceleration measurements were then compared with the theoretical values derived from the numerical simulations to assess the consistency of the results. This comparison provided a direct validation of the model predictive capabilities. The experimental apparatus was constructed using lightweight materials – plastic, cylindrical containers and flexible connectors (Table 1), which were carefully selected to ensure the accurate simulation of the intended system dynamics. The authors intention when selecting the materials was to provide instrumentation that does not change or affect the dynamics of the system being tested. The experimentally designed system serves as a representation of the theoretical model and numerical investigations presented within this article. The primary objective of the experimental research is not only to validate theoretical assumptions but, above all, to confirm the practical feasibility of implementing the proposed solution in engineering applications.

Table 1
Aluminium profile property

Property	Value
Length	500 mm
Cross-section	40×40 mm
Mass	0.87 kg

4.2. Results of experimental and numerical studies

In order to validate the correctness of the test stand operation, experimental tests were carried out for one exemplary mass configuration and some different values of excitation frequencies. The tests were performed for the frequency of the excitation equals 2.27 Hz and 2.47 Hz. The values were chosen as being above the system natural frequency they allowed for a nonresonant and controllable conditions of the experiment. These frequencies ensured stable system behaviour and enabled a meaningful comparison between experimental and simulation results. The analysed time span is approximately 10 seconds, and the sampling frequency is 128.2 Hz.

The measuring scheme comprises an excitation source, the investigated system is equipped with the PTMD and a data acquisition system for monitoring the dynamic response. The primary objective is to analyse the propagation of vibrations

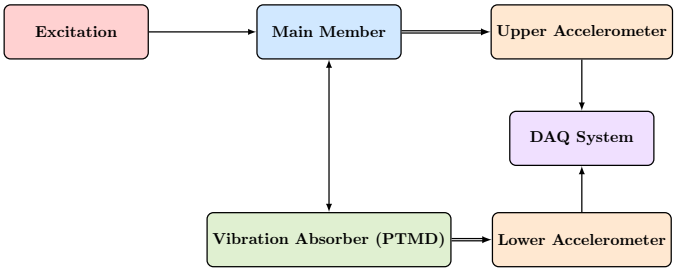

Fig. 5. Scheme of the measuring system used during the experimental tests

through the system and evaluate the effectiveness of the PTMD in attenuating structural oscillations.

The system is subjected to controlled dynamic excitation, and its response is recorded at critical locations to assess the interaction between the main structural member and the PTMD. Given the importance of this interaction, two accelerometers are strategically positioned:

- **Upper accelerometer** – mounted on the main structural member near the excitation source, capturing the structural response before energy is transferred to the PTMD,
- **Lower accelerometer** – positioned adjacent to the PTMD, measuring the localised vibrational response and quantifying the absorber efficiency in vibration attenuation.

Both accelerometers send their measured signals to a data acquisition (DAQ) system. The DAQ system is connected to a computer, where the collected data is processed using specialised software for signal processing and analysis, frequency response evaluation, and performance assessment of the vibration absorber.

Figure 6 presents two waveforms of the main pendulum member acceleration in time domain. Further one can observe a frequency domain representation of the signals enabling a clearer results interpretation. Figures show the results of the numerical simulations for experimental test conditions. Similarly as for the experimental part, the results of numerical simulation are presented in time domain in Fig. 7 for corresponding frequencies as a comparative case.

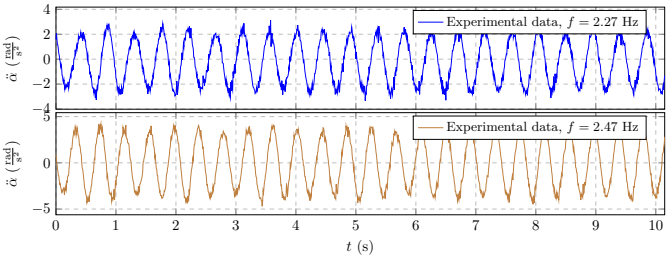

Fig. 6. Experimental data for acceleration of pendulation of the main member of double pendulum

To improve clarity and facilitate interpretation, one has grouped the results by identical excitation frequency values f and combined the corresponding figures to display both associated waveforms. This restructuring enhances the overall readability of the results and enables a more direct comparison of

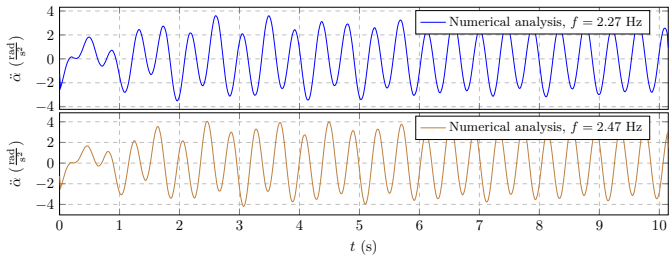

Fig. 7. Validation analysis for acceleration of pendulation of the main member of double pendulum

the system response under the same excitation conditions. As a result, the analysis becomes more comparative in nature, allowing for easier identification of patterns and more straightforward formulation of conclusions.

Table 2
PET container parameters

	Container parameter
Diameter	94.4 mm
Height	317 mm
Neck fish	28 mm PCO 1810
Volume	1.5 l

The comparison of numerical simulations presented in Figs. 8 and 9 with experimental data at excitation frequencies of 2.27 Hz and 2.47 Hz reveals clear insights into the dynamic behaviour of the system. At 2.27 Hz, the system exhibits a gradual build-up of oscillations, with a noticeable transient response in the initial seconds before settling into a steady-state regime. The amplitude of angular acceleration remains relatively modest, reaching approximately ±3.5 rad/s^2. In contrast, the response at 2.47 Hz is characterised by significantly higher amplitudes, exceeding ±4.5 rad/s^2, and a more rapid transition into steady-state oscillations. This behaviour indicates that 2.47 Hz is closer to the system natural frequency, resulting in a more efficient energy transfer from the excitation input – consistent with resonance phenomena. Despite the presence of noise in the experimental measurements, the underlying periodicity of the system motion is well-preserved and shows strong agreement with the numerical predictions, particularly in the steady-state regime. The model captures both the phase and amplitude evolution with notable accuracy across both cases. The close alignment between the experimental and simulated results validates the predictive capability of the proposed mathematical model and confirms its suitability for analysing the system response under varying excitation conditions.

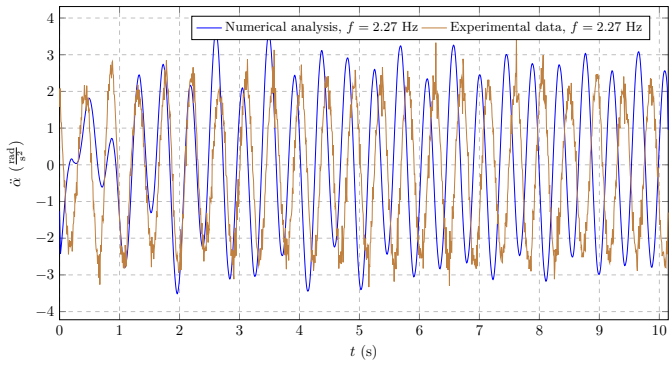

Fig. 8. Comparative results for acceleration of pendulation of the main member of double pendulum for excitation frequency 2.27 Hz

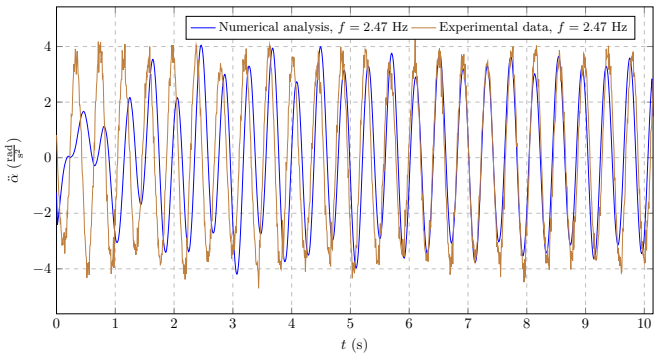

Fig. 9. Comparative results for acceleration of pendulation of the main member of double pendulum for excitation frequency 2.47 Hz

For further confirmation that the amplitude values are not greater for the PTMD member, the corresponding results have been analysed and presented in both, the time (Fig. 10) and frequency domain (Fig. 11).

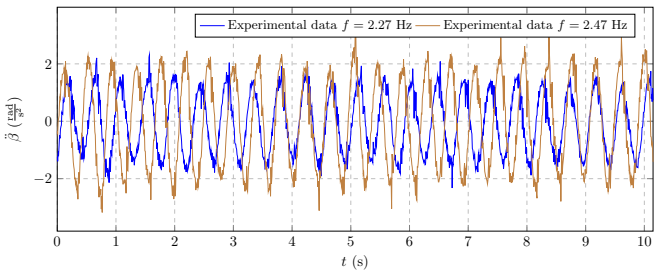

Fig. 10. Experimental data for acceleration of pendulation of the PTMD

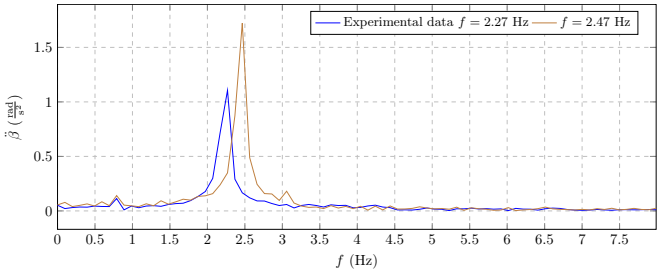

Fig. 11. Spectra for experimental data for acceleration of pendulation of the PTMD

4.3. Comparative study on experimental and numerical results

It should be noted that Fig. 12 presents only the response spectra of the main pendulum member (the attenuated system), whereas Fig. 11 shows the spectra corresponding to the second pendulum member.

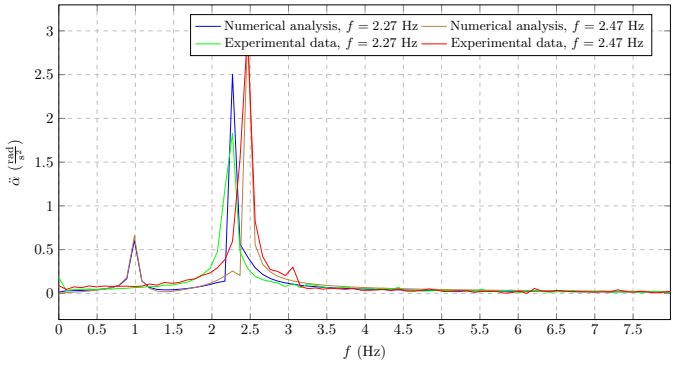

Fig. 12. Comparative spectral analysis for the numerical and experimental model

The spectral analysis presented in figure 12 depicts two system response bands of different frequencies that indicate different values of vibration amplitudes (vibration acceleration peaks) for the two different excitation frequencies. The vibrations of a lower frequency are characterised by a lower amplitude, while vibrations of a higher frequency are characterised by a higher amplitude value. The comparative analysis of the spectral characteristics prepared based on the results of experimental research and the results of numerical simulations allows to state their qualitative consistency. The individual spectral fringes correspond to similar values of the vibration frequencies of the experimental tests, where the lower is 2.27 Hz and higher 2.47 Hz. The values of the excitations are shifted between each other by 0.2 Hz in the frequency domain. In case of numerical simulations, it can be noticed that the lower frequencies of excitations are characterised by the higher values of system vibration amplitudes than in case of experimental tests. Respectively, for the simulation the amplitude value equals to 2.5 rad/s^2 and for the experimental results 1.83 rad/s^2. However, as the frequency of vibrations increases, their amplitudes reach the same value in the simulation and experiment and is equal to 2.99 rad/s^2. A clear similarity of the waveforms obtained confirms the consistency of the numerical model and the model for experimental study.

5. NUMERICAL STUDY – RESEARCH RESULT

5.1. Influence of a damping coefficient value

It is important to note that all results presented within this section are based solely on numerical simulations provided by the proposed mathematical model. The simulation results were obtained for a total duration of 300 seconds. However, the simulations demonstrate that the system exhibits stable behaviour within the initial 100 seconds. For clarity, the presented results have been shortened, as they follow the same trend of limiting amplitude values, which is already evident in the initial phase. Therefore, only the initial stage of vibrations is presented to concisely illustrate the key effects. It is also noteworthy that the time interval of 100 seconds corresponds to approximately 15 cycles of external excitation (300 seconds – approximately 45 cycles). To facilitate interpretation and highlight the evolution of the system behaviour with respect to the periodic input, the simulation results are presented as a function of the number of excitation cycles rather than physical time.

The influence of a drag coefficient value on the system dynamic response under harmonic excitation is presented in Fig. 13. The analysis takes into account several values of damping ratios from 0 to 20 N s/rad. Such an analysis allows us to determine the value of system resistance, which provides stable dynamics corresponding to the real values of amplitudes for both of the pendulum arms.

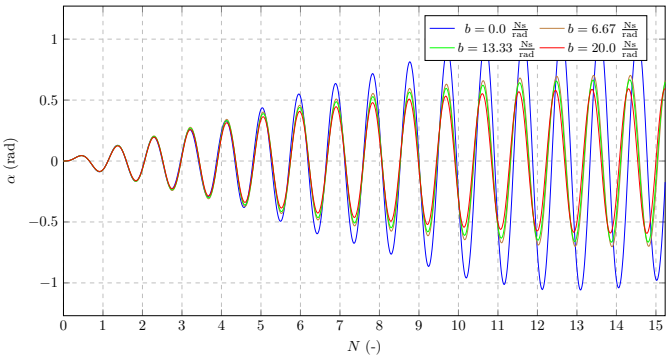

Fig. 13. Pendulation of the main member of the double pendulum under the influence of various damping coefficient values – direct comparison

A significant impact of the investigated parameter was observed based on the carried out simulations. It can be stated that exists some threshold value, where the system response reaches asymptotical stability (lack of the amplitude overloading). For the assumed parameters it is about 10 N s/rad, which was selected for further analyses. The extreme amplitude values are considered in range of −1.06 rad to 1.06 rad. Due to the nature of the phenomenon, the process requires to identify an appropriate level of damping, therefore the choice of the drag coefficient value needs to be highlighted as it is fundamental to obtain a reliable system response.

5.2. Influence of an activation time

An analysis of the absorber activation time was conducted based on the results of previous simulations. For the investigation purposes, the same parameters of the system were decided to be used. The solutions are presented in Fig. 14. The activation

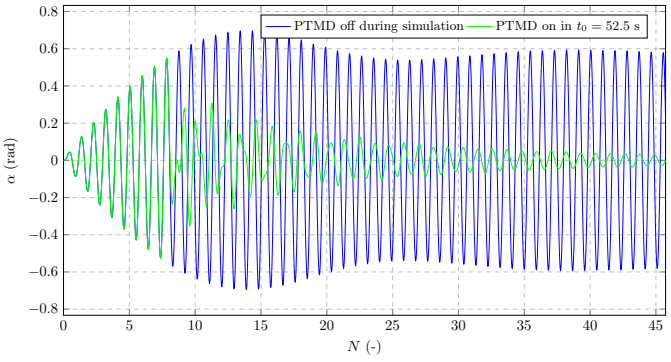

Fig. 14. Amplitude of pendulation (angular displacement) of the main pendulum member $\alpha(t)$ under the influence of varying activation time

times used in the analysis were set to 52.5 s. The authors planned to show the system dynamic behaviour in dependence on time, when the PTMD was disabled and turned on and the main focus was put on values of the amplitudes during the mass transfer.

It is worth noting that activation time conditions will inevitably vary across different systems, depending on their specific design parameters, operating environments, and performance requirements of the absorber. Therefore, having a specified implementation of the absorber defining these conditions is crucial to ensure that the activation is precisely aligned with each system unique constraints and functional objectives (allowable level of vibrations amplitude or signal energy), in order to ensure the system functions effectively. In Fig. 14, the activation time was set for demonstration purposes, allowing for an immediate limitation of amplitude values. This simplification serves to illustrate the fundamental concept but does not necessarily represent the conditions required for a fully optimised system.

The obtained numerical simulations enable to evaluate the role of impact of the activation time t_0 on the overall amplitude level of vibrations. It can be concluded that an earlier activation of the device prevents from further evolution of resonant vibrations. In Fig. 14 one can observe the effect of stabilisation of amplitudes in some time after transfer of the fluid. The observations allow us to propose a simplified design method, which is based on the operation of the main system (before the activation) and the coupled system that consists of the damper-filled and main member. It can be concluded that the operation of the attenuator not only controls the amplitude vibrations (quantitative changes) but also significantly changes the dynamics in its qualitative aspect. It is obvious that a later damping activation causes higher level of vibrations, which when uncontrolled can affect the system negatively.

5.3. Influence of a transferred fluid amount

It is worth noting that there may also be additional phenomena worth investigating in connection with liquid transfer dynamics, such as flow-induced instabilities. From a scientific and engineering standpoint, it is indeed worth investigating the influence of liquid transfer speed on vibration damping. Such analysis can uncover optimal operational parameters, including flow rates that lead to minimise vibration amplitudes, thereby improving system performance, durability, and safety. That said, the impact of flow speed is highly dependent on the specific system to which the absorber is applied. Based on current simulations and experimental setup, one suspects that for systems of a similar scale to the one examined, the liquid transfer speeds will remain relatively low, and therefore are unlikely to introduce significant dynamic effects such as sloshing or strong fluid-structure coupling. However, this influence may become more pronounced especially when the scale of application increases, and should therefore be carefully evaluated in the context of larger or more complex systems.

At this stage, the analysis of the amount of a transferred water mass was performed. The solutions in time domain are presented in Fig. 15. The investigated parameter was limited within the range of 0.0 kg to 5 kg. The carried out investigation was prepared for 7 simulations. The main objective was to study the influence of the transferred mass on the absorber efficiency, especially the values of amplitudes during the mass transfer and steady vibrations were carefully followed.

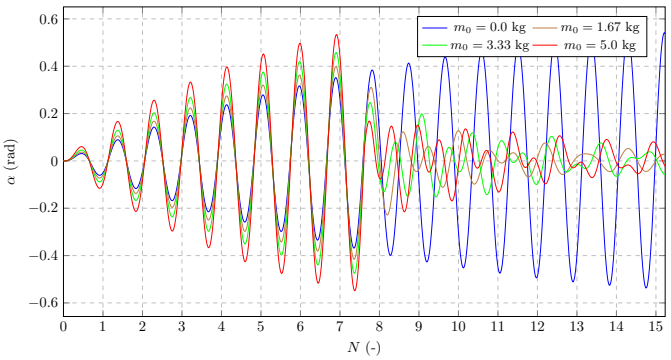

Fig. 15. Pendulation of the main member of the double pendulum in dependence on various masses of the transferred liquid – direct comparison

The performed simulations show the impact of transferred mass m_0 on the overall amplitude level of vibrations. Based on the presented results, it can be stated that some specified amount of the transferred fluid can prevent the system pendulation from evolution of resonant vibration. It is worth mentioning that the mass of fluid needed to decrease probability of resonance occurrence can be found as reasonable related to the mass of the considered system. In Fig. 15 one can observe an immediate response of the system to the start of the water mass transfer. It needs to be highlighted that additional mass of the damping medium causes higher dynamics of the initial system response. Therefore, the mass of the fluid to be transferred to control or damp the vibrations should be carefully calculated having in mind a relation to the total mass of the system and an increase in the initial amplitude of the response when the system includes the absorber. However, based on the results obtained, the proposed solution seems to fulfil the assumptions regarding the vibrations control. It can be observed that there exists some threshold value of the mass to be transferred, which when exceeded does not cause any significant changes regarding the quantitative results. A meaningful difference in change of m_0 value is visible between the first (blue) and second (orange) spectrum, where their mutual relation of the maximum values of the amplitudes is almost twice.

5.4. Absorber dynamics under influence of a liquid mass transferred

It is also worth analysing the influence of the transferred water mass on dynamics of the pendulum second member found in this system as a vibration attenuator. The analyses performed in time domain are depicted in Fig. 16. Studying the obtained results it should be noticed that the additional mass (the water inside the pendulum members) introduced to the system being utilised as vibration controller causes the increase of energy in the system, which is manifested in higher amplitudes of vibrations of the second pendulatory member before the activation. However, the

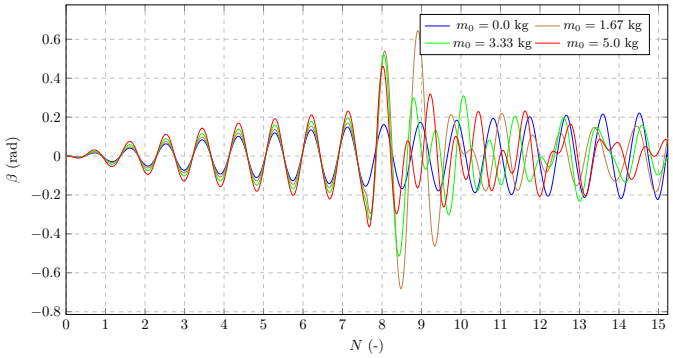

Fig. 16. Pendulation of the second member of the double pendulum in dependence on various masses of the transferred liquid – direct comparison

greater the mass of the transferred water, the lower the overall level of vibrations in the system.

Regardless of the initial increase of the amplitude values of the pendulum second member, when the water mass starts to be transferred, the pendulation amplitudes reach and oscillate at the very similar values as the ones of the main pendulum not exceeding the maximum value of 0.32 rad.

6. ASSESSMENT OF THE EFFECTIVENESS OF THE ABSORBER OPERATION

6.1. Summary of the absorber effectiveness

An evaluation of the effectiveness of the proposed absorber was carried out to prove the presented approach (technical solution) is interesting from the point of view of vibration control. The effectiveness of the absorber is evaluated as a percentage by comparing the maximum vibration response in each scenario (10 simulation cases considered, beginning with the scenario where the absorber is active and ending with the scenario where the absorber is disabled) to the highest recorded vibration amplitude – absorber disabled. The effectiveness is calculated by taking the ratio of each scenario's peak response to the maximum, subtracting it from one to express the reduction in vibration. A value close to 100% indicates that the absorber significantly mitigates vibrations, effectively reducing the response to nearly 0. Conversely, a value near 0% suggests that the absorber has little to no influence on vibration suppression, while negative values, if present, would indicate an increase in vibrations rather than a reduction. Overall, this assessment can be expressed as:

$$\Delta = 100 \cdot \left(1 - \frac{A_{\max_{\text{case}}}}{A_{\max}}\right) \quad [\%]. \tag{18}$$

It was decided to investigate different activation times of the absorber, where the parameter span is from −30 to 300 s. The numerical analyses were performed for 10 simulation cases. The extreme values of parameters represent the best and the worst operational efficiency of the absorber. The most efficient operation corresponds to activation time of −30 s before the resonant zone occurs, while the worst absorber operation reflects the device activation when the simulation is already finished. The results are shown in Fig. 17.

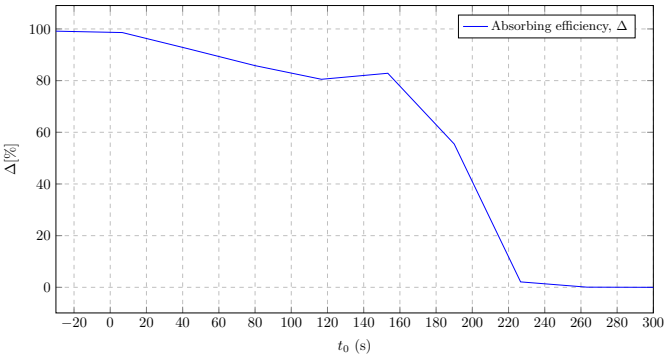

Fig. 17. Absorber effectiveness assessment in dependence on activation time

The performed simulations revealed high effectiveness of the proposed concept for shorter activation times. The best result may be achieved while the absorber activation is set before the system start-up time (before the system operation or predicted resonant vibration). Nevertheless, it is not possible to eliminate the amplitude related to the existence of a residual value due to viscous damping, which is needed for the proper working of the proposed concept. The simulation tests show that if the activation time is under 60 seconds, it can be stated that the absorber operates under its optimal conditions. The differences between the best result and the cases for which the activation times are lower than 60 seconds are almost the same. This proves the usefulness of the presented concept.

In order to ensure sufficiently rapid mass variation, it is indeed necessary to implement a control system that enforces a specific flow rate profile – such as those illustrated in Figs. 2 and 3 – with appropriate parameters. As such, these flow curves are not arbitrary but must be actively imposed through a dedicated controller. It is worth noting that the shape and parameters of the flow profile play a critical role, and future work will focus on analysing various control strategies, parameter variations, and flow curve shapes to further optimise the system performance.

7. SWEEP FREQUENCY ANALYSIS

7.1. Transferred mass impact

In order to confirm the effectiveness of the proposed concept, this section presents comparative studies between a traditional, passive-tuned mass damper (TMD) against the proposed idea of a semi-active PTMD. To confirm its performance the following presents the system dynamics under various operating conditions. Since all previously presented simulations are based on comparisons done for discrete frequencies, the authors prepared analyses based on a continuous change of frequency during the operation for a transferred mass and activation time impact on the system lasting over 16 minutes. The conducted frequency sweeps were performed to ensure a sufficiently fine resolution in order to draw strong conclusions regarding whether resonance might be controlled by the liquid overflow.

The performance of the system was compared against a tuned mass damper where no varying mass was included. The system presented in Fig. 1 represents the reference system being studied but the masses of the system m_α and m_β remain constant. The system linearised governing equations are presented in (19), (20).

$$b\dot{\alpha} + l_\alpha^2\left(\dot{m}_\alpha + \dot{m}_\beta\right)\dot{\alpha} + l_\alpha^2\left(m_\alpha + m_\beta\right)\ddot{\alpha} - l_\alpha\left(-gm_\alpha - gm_\beta\right)\alpha + l_\alpha l_\beta\dot{\beta}\dot{m}_\beta + l_\alpha l_\beta m_\beta\ddot{\beta} = T_0\sin(\Omega t), \tag{19}$$

$$b\dot{\beta} + l_\beta^2\dot{\beta}\dot{m}_\beta + l_\beta^2 m_\beta\ddot{\beta} + gl_\beta\beta m_\beta + l_\alpha l_\beta\dot{\alpha}\dot{m}_\beta + l_\alpha l_\beta m_\beta\ddot{\alpha} = 0, \tag{20}$$

where g is the acceleration of gravity, α is the angle of the upper pendulum swing, β is the angle of the lower pendulum swing, $\dot{\alpha}$ is the generalised velocity of the upper pendulum member, $\dot{\beta}$ is the generalised velocity of the lower pendulum member, l_α is the length of the upper pendulum, l_β is the length of the lower pendulum, m_α is a constant mass of the upper pendulum and m_β is a constant mass of the lower pendulum. Due to the fact that a traditional PTMD does not use the phenomenon of fluid flow, the masses of the system remain constant and, consequently, the equations describing the motion of the system take a different form – they are much simpler because they do not take into account the derivatives of the time-varying mass. The coupling between the equations of motion in the referenced system is realised by its accelerations ($\ddot{\alpha}(t)$, $\ddot{\beta}(t)$). A clear difference between the system proposed and the traditional PTMD can be seen in the system damping matrices. Comparing the equation (14) and (23) it is obvious that the phenomenon of varying mass introduces additional components into the damping matrix to cause changes in the system dynamics towards smaller, damped values of velocity and then displacement amplitudes.

$$\mathrm{M} = \begin{bmatrix} l_\alpha^2\left(m_\alpha + m_\beta\right) & l_\alpha l_\beta m_\beta \\ l_\alpha l_\beta m_\beta & l_\beta^2 m_\beta \end{bmatrix}, \tag{21}$$

$$\mathrm{K} = \begin{bmatrix} l_\alpha\left(gm_\alpha + gm_\beta\right) & 0 \\ 0 & gl_\beta m_\beta \end{bmatrix}, \tag{22}$$

$$\mathrm{C} = \begin{bmatrix} b & 0 \\ 0 & b \end{bmatrix}. \tag{23}$$

Root of numerator of this formula provides tuning condition for initial parameters of the investigated concept. The adaptive PTMD is tuned on excitation frequency if entire fluid is pumped to the absorber. Mass ratio was initially selected as 0.2 for further numerical investigation of the proposed concept. At this stage of the investigation (that can be termed as proofing of concept) it was no need to look for optimal parameters of resonance mitigation so this problem was not considered. However, a wide spectrum of numerical investigation allows for a raw selection of damping in the analysed concept. Performed simulations and empirical verification proof correctness of the presented idea so it allows to state that further investigation (also in a field of optimal selection of absorber parameters) is intentional and reasonable.

Numerical simulations are performed based on the same parameters for both of the analysed systems. The numerical data are presented in Table 3. The rate of change of frequency was set to 0.001 rad/s.

Table 3
Numerical data

Parameter	Value
γ	$\frac{1}{2} - \arctan\left(\frac{\lambda(t-t_0)}{\pi}\right)$
l_α, l_β	$9 \pm 2\cdot(1-\gamma)$ m
m_α, m_β (pipe)	$\mp m_0\gamma$ kg
g	9.81 m/s^2
m_α (attenuated object)	10 kg
m_β (PTMD)	0.1 kg
T_0	18 Nm
λ	100
m_0	2 kg

A comparison of effectiveness and performance assessment of the systems are presented in the following numerical simulations.

The analyses are prepared for two scenarios – two different masses of the liquid overflow for two types of devices – traditional TMD and PTMD with the transferred mass. Figure 18 presents pendulation amplitude of the main member over 1000 s for instantaneously changed frequency (up to 1 rad/s. Based on the results in time domain, it is already observable that despite the initial slight increase in the amplitude for the system with the absorber, the liquid overflow causes a significant reduction in the amplitude values especially in range of the second resonance frequency slightly shifting the limited resonance towards lower frequency values. The mass transferred in the case was $m_0 = 2$ kg and the absorber was activated at 550 s.

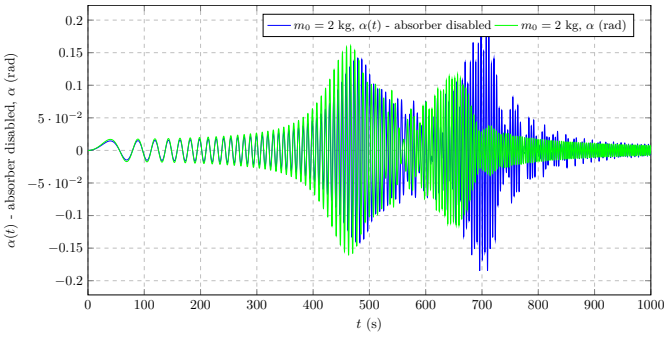

Fig. 18. Sweep frequency analysis – angular displacement $\alpha(t)$ amplitude values for the system with and without PTMD

The frequency spectrum presented in Fig. 19 confirms the observations made in time domain signals. The amplitude values are fairly limited for a wide range of the system operation and the second resonance frequency was shifted.

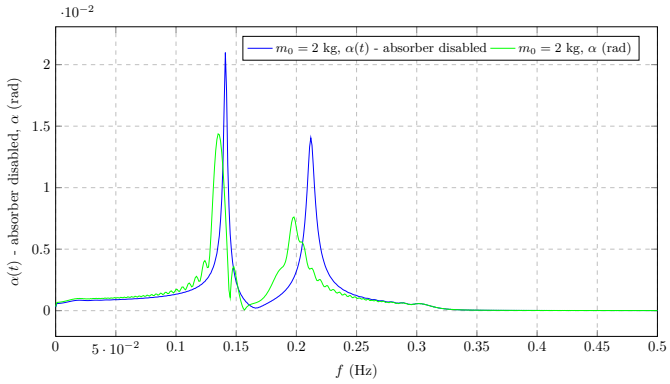

Fig. 19. Sweep frequency analysis in spectral domain – angular displacement $\alpha(t)$ amplitude values for the system with and without PTMD

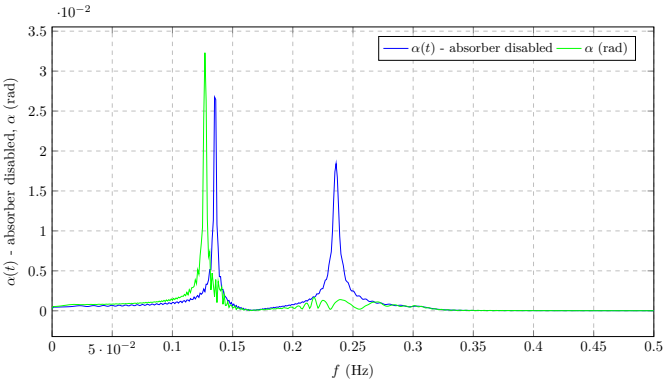

Fig. 21. Sweep frequency analysis in spectral domain – angular displacement $\alpha(t)$ amplitude values – impact of absorber activation in 700 s

7.2. Activation time impact

The next case study presents a scenario when the transferred mass was changed up to 5 kg (Fig. 20). That naturally caused the resonance zone to occur at a different time interval and amplitude range comparing to the previously considered case. The absorber was activated in 700 s of the pendulum motion and as can be observed it completely damped the zone of resonant vibrations, causing a linear decrease in the value of the pendulum vibration amplitudes.

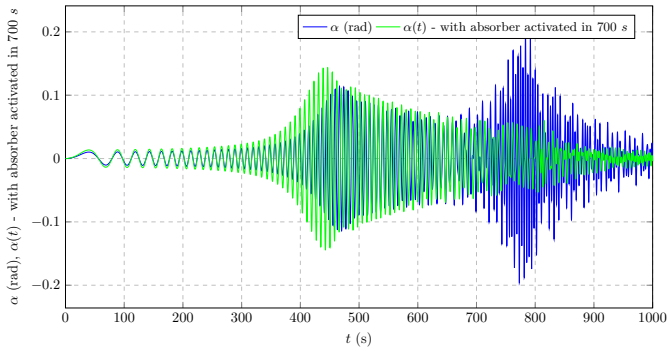

Fig. 20. Sweep frequency analysis – angular displacement $\alpha(t)$ amplitude values – impact of absorber activation in 700 s

The frequency spectrum presented in Fig. 21 confirms the observations made in time domain signals. The second resonant frequency was damped completely whilst the first harmonic got a little bit higher amplitude value. However the value is of an insigniificant change and can be ommitted in considerations. Examining the structure it is crucial to assess how the attenuator works during the most dangerous states – around/in resonant zones, as the device was created to mitigate or eliminate the formation of such vibrations completely if possible. Based on the varying speed during the analysis, frequency sweep was additionally conducted at discrete frequencies and a frequency response function (FRF) of the system was generated and presented in Fig. 22.

Figures 23 and 24 represent the envelopes of the amplitude responses of vibrations shown in Figs. 18 and 20 for the model in-

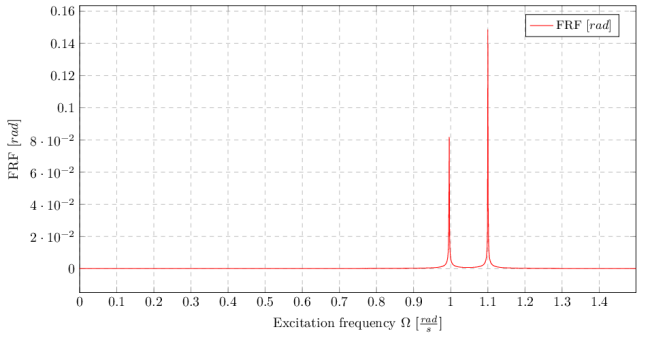

Fig. 22. PTMD frequency response function

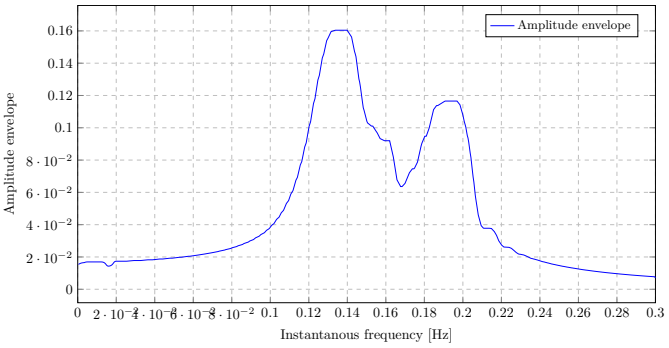

Fig. 23. Amplitude of vibration of $\alpha(t)$ while sweeping the excitation frequency

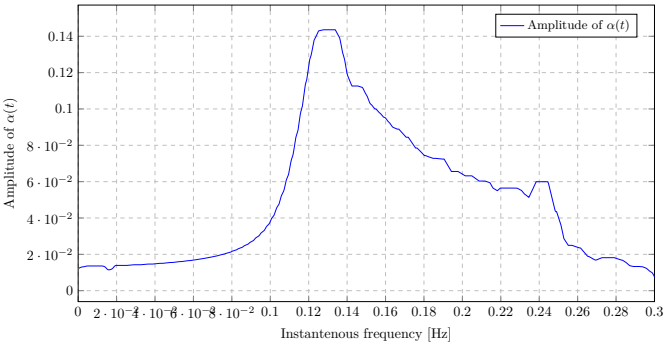

Fig. 24. Amplitude of vibration of $\alpha(t)$ while sweeping the excitation frequency and PTMD device attached to the system

corporating PTMD. Thus, the envelopes in Figs. 23 and 24 capture the transition from the transient oscillatory region through resonant vibrations to the steady-state harmonic motion, emphasising the dual dynamic behaviour of the system. The role of the PTMD is to mitigate the transient amplitude peaks and reduce vibration at the resonant frequencies, ultimately facilitating the system stabilisation into steady-state motion.

Two resonance zones can be observed in the amplitude envelope curves that can be used to create a control algorithm that in the future will allow us to avoid high-amplitude vibrations ensuring dynamics in the desired conditions.

8. CONCLUSIONS

Concluding the paper, it is assumed that the presented concept utilising the varying mass distribution can be applied as a semi-active damping vibration system and hence that it allows for effective control of dynamics of the considered object with utilisation of actuators, whose energy of activation is relatively small. This approach, as proven within this article allowed us to demonstrate the impact on system dynamic response and the object reaction (time histories and spectra) and its sensitivity to amount of the transferred liquid.

In the paper the authors proposed a mathematical model of the structure and the absorber attached. Numerous complex analytical and numerical computations, including a sensitivity analysis, were performed in order to fully investigate the proposed phenomenon and confirm that the mass exchange in the system can be successfully implemented as an effective method of vibration attenuation. This statement was verified, proven and confirmed on the basis of numerical and experimental studies.

It can be stated that activation time plays a crucial role in the process based on the carried out simulations. In-depth analysis of the obtained result allows us to state that the shorter activation time, the lower maximum amplitude reached in given period. The detuner effectiveness assessment shows the best performance for low activation times as presented in Fig. 17. It implies that the proper selection of starting of transfer time ensures the desired value of maximal vibration amplitude. The obtained results allow us to design new strategies of vibration absorption.

Based on the performed activities, the following conclusions can be stated and should be underlined:

- The proposed solution is a semi-active vibration control system that does not require a high amount of energy to achieve a regulation error likely acceptable for systems of comparable scale and dynamic characteristics; however, the precise tolerance for regulation error should be determined based on the specific performance requirements of the intended application.
- Analysis of the damping values applied shows that below 7 N s rad^{-1} the system response does not depend significantly on the damping value.
- The results of the analytical investigation enable us to conclude that the examined ratios of the transferred to total mass give an applicable effect of the proposed solution – for all of the investigated cases the value was between 10–15%.
- 15% of the transferred mass of the entire system ensures the lowest dynamic response of the main member.
- The presented model of a double mathematical pendulum provides a reasonable approximation for analysing the system dynamics, with a good agreement to experimental results, the values before and after the change were consistent with the proposed simplified model, only transient zone revealed inconsistency.
- Experimental tests carried out confirmed the effectiveness of the presented modelling procedure.
- The comparative study between numerical and experimental investigation reveals some discrepancies in vibrational spectra, the extra frequency peak comes from natural oscillation of the system, which was not ensured in the test setup.
- The overall efficiency of the proposed solution depends on the specific case and the appropriate selection of parameters; based on the conducted simulations, it can be estimated that for the largest mass considered, the reduction in amplitude values reaches up to 15–20%.
- The minimal value of the viscous drag ensures stable system behaviour and provides fast enough decay time (both eigenvalues have negative real parts due to drag. The presence of an imaginary component in the eigenvalues (corresponding to the natural frequencies discussed in Section 3.2) indicates that the system's free vibration decays to zero).
- The spectral analysis in the field of numerical simulations of the system dynamic behaviour performed when the PTMD is activated showed the spectra containing harmonical components of the excitation and natural frequencies, which confirms correctness of the proposed approach.

The advantage of the proposed solution is seen in the utilisation of a simple physical model, the operational range of which was extended based on the principle of operation of TMD devices, using the variability of the system parameters. Additionally, the method (absorber) of vibration damping can be successfully used wider than popular magnethoreological fluids, the application of which, depending on operational conditions, is not always possible.

The demonstrated detuner works as a tuned mass damper but the proposed concept is able to change its parameters during the operation. The performed simulations confirm the system is sensitive to changes of TMD parameters. It facilitates new control strategies for systems containing fluids as a part of the entire structure, e.g., water towers, oil rigs or pipelines. For these structures there is a possibility of the utilisation of the structure features to damp vibrations by a change of mass distribution with application of the proposed device (method).

The presented innovative vibration damping method has the potential for effective application across various industrial sectors. In industrial machinery, it can be employed to eliminate mechanical vibrations by dynamically adjusting the pendulum mass. In buildings, it will serve to reduce vibrations, while in vehicles, it aims to enhance travel comfort. In the construction of bridges or wind towers, these systems will effectively minimise the impact of vibrations on the structure, adapting to variable environmental conditions. This approach represents a significant stride towards the practical implementation of advanced vibration control methods in real engineering scenarios.

REFERENCES

[1] C. Cempel, *Vibroacoustic condition monitoring*. Ellis Horwood New York, 1991.

[2] S. Elias and V. Matsagar, "Research developments in vibration control of structures using passive tuned mass dampers," *Annu. Rev. Control*, vol. 44, pp. 129–156, 2017, doi: 10.1016/j.arcontrol.2017.09.015.

[3] E. Diez-Jimenez, R. Rizzo, M. Gómez-García, and E. Corral-Abad, "Review of passive electromagnetic devices for vibration damping and isolation," *Shock Vib.*, vol. 11, p. 1250707, 2019, doi: 10.1155/2019/1250707.

[4] R. Lewandowski, *Reduction of vibration of civil engineering structures*. Wydawnictwo Naukowe PWN, 2014.

[5] S. Sarkar and A. Chakraborty, "Development of semi-active vibration control strategy for horizontal axis wind turbine tower using multiple magneto-rheological tuned liquid column dampers," *J. Sound Vib.*, vol. 457, pp. 15–36, 2019, doi: 10.1016/j.jsv.2019.05.052.

[6] B. Xu, C. Xiang, Q. Yechen, D. Peng, and D. Mingming, "Semi-active vibration control for in-wheel switched reluctance motor driven electric vehicle with dynamic vibration absorbing structures: Concept and validation," *IEEE Access*, vol. 6, pp. 60 274–60 285, 2018, doi: 10.1109/ACCESS.2018.2875197.

[7] M. Gutierrez Soto and H. Adeli, "Semi-active vibration control of smart isolated highway bridge structures using replicator dynamics," *Eng. Struct.*, vol. 186, pp. 536–552, 2019, doi: 10.1016/j.engstruct.2019.02.031.

[8] J. Allien, H. Kumar, and V. Desai, "Semi-active vibration control of sic-reinforced al6082 metal matrix composite sandwich beam with magnetorheological fluid core," *Proc. Inst. Mech. Eng. Part L-J. Mater.-Des. Appl.*, vol. 234, pp. 408–424, 2019, doi: 10.1177/1464420719890374.

[9] J. Kawęcki and R. Masłowski, "Use of passive, quasi-active and hybrid silencers to reduce seismic and paraseismic vibrations of buildings - overview of solutions," *Tech. Trans. Civ. Eng.*, vol. 3-B/2010, no. 11, pp. 59–67, 2010, doi: 10.1051/matecconf/201925403003.

[10] A. Hashemi and P. Quenneville, "Large-scale testing of low damage rocking cross laminated timber (clt) wall panels with friction dampers," *Eng. Struct.*, vol. 206, p. 110166, 2020, doi: 10.1016/j.engstruct.2020.110166.

[11] S. Elias and V. Matsagar, "Wind response control of tall buildings with a tuned mass damper," *J. Build. Eng.*, vol. 15, pp. 51–60, 2018, doi: 10.1016/j.jobe.2017.11.005.

[12] C. Li, H. Pan, and L. Cao, "Pendulum-type tuned tandem mass dampers-inerters for crosswind response control of super-tall buildings," *J. Wind Eng. Ind. Aerodyn.*, vol. 247, p. 105706, 2024.

[13] F. Ismail, J. Tanjung, and S. Aruan, "On the use of a simple tuned mass damper model for reducing the excessive vibration of tsunami evacuation suspension footbridge," *MATEC Web Conf.*, vol. 229, p. 01013, 2018, doi: 10.1051/matecconf/201822901013.

[14] J. Guimarães, M. dos Reis Farias, M. César, and R. Carneiro de Barros, "Dynamic analysis of wind tower and dimensioning of tuned mass damper," *Revista de Engenharia e Pesquisa Aplicada*, vol. 6, no. 2, pp. 55–64, 2021.

[15] M. Ghassempour, G. Failla, and F. Arena, "Vibration mitigation in offshore wind turbines via tuned mass damper," *Eng. Struct.*, vol. 183, pp. 610–636, 2019, doi: 10.1016/j.engstruct.2018.12.092.

[16] H. Gao, C. Wang, C. Huang, W. Shi, and L. Huo, "Development of a frequency-adjustable tuned mass damper (fatmd) for structural vibration control," *Shock Vib.*, vol. 2020, p. 9605028, 2020, doi: 10.1155/2020/9605028.

[17] W. Shi, L. Wang, and Z. Lu, "Study on self-adjustable tuned mass damper with variable mass," *Struct. Control Health Monit.*, vol. 25, p. e2114, 2017, doi: 10.1002/stc.2114.

[18] Y. Xiang, P. Tan, H. He, H. Yao, and X. Zheng, "Pendulum tuned mass damper (ptmd) with geometric nonlinear dampers for seismic response control," *J. Sound Vib.*, vol. 570, p. 118023, 2024.

[19] Y. Xiang, P. Tan, H. He, Q. Chen, Y. Zheng, and Y. Li, "Seismic optimization of pendulum tuned mass damper with hysteretic damping," *Int. J. Mech. Sci.*, vol. 269, p. 109073, 2024.

[20] L. Wang, S. Nagarajaiah, W. Shi, and Y. Zhou, "Semi-active control of walking-induced vibrations in bridges using adaptive tuned mass damper considering human-structure-interaction," *Eng. Struct.*, vol. 244, p. 112743, 2021, doi: 10.1016/j.engstruct.2021.112743.

[21] L. Wang, W. Shi, Q. Zhang, and S. Nagarajaiah, "Study on adaptive-passive multiple tuned mass damper with variable mass for a large-span floor structure," *Eng. Struct.*, vol. 209, p. 110010, 2020, doi: 10.1016/j.engstruct.2019.110010.

[22] L. Wang, S. Nagarajaiah, W. Shi, and Y. Zhou, "Seismic performance improvement of base-isolated structures using a semi-active tuned mass damper," *Eng. Struct.*, vol. 271, p. 114963, 2020, doi: 10.1016/j.engstruct.2022.114963.

[23] L. Wang, Y. Zhou, and W. Shi, "Seismic response control of a nonlinear tall building under mainshock–aftershock sequences using semi-active tuned mass damper," *Int. J. Struct. Stabil. Dyn.*, vol. 23, p. 16n18, 2023, doi: 10.1142/S0219455423400278.

[24] M. Rahman, Z.C. Ong, S. Julai, M.M. Ferdaus, and R. Ahamed, "A review of advances in magnetorheological dampers: their design optimization and applications," *J. Zhejiang Univ.-Sci. A*, vol. 18, pp. 991–1010, 2017, doi: 10.1631/JZUS.A1600721.

[25] Y.M. Khedkar, S. Bhat, H. Adarsha, Y.M. Khedkar, S. Bhat, and H. Adarsha, "A review of magnetorheological fluid damper technology and its applications," *Int. Rev. Mech. Eng.*, vol. 13, pp. 256–264, 2019, doi: 10.15866/IREME.V13I4.17224.

[26] Q. Guo, X. Yang, K. Li, and D. Li, "Parameters identification of magnetorheological damper based on particle swarm optimization algorithm," *Eng. Appl. Artif. Intell.*, vol. 143, p. 110016, 2025.

[27] C. Snoun and M. Trigui, "Design parameters optimization of a particles impact damper," *Int. J. Interact. Des. Manuf.*, vol. 12, p. 1283–1297, 2018, doi: 10.1007/s12008-018-0463-y.

[28] L. Zheng, W. Zixin, F. Sami, and L. Xilin, "Particle impact dampers: Past, present, and future," *Struct. Control Health Monit.*, vol. 25, p. e2058, 2017, doi: 10.1002/stc.2058.

[29] L. Gagnon, M. Morandini, and G. Ghiringhelli, "A review of particle damping modeling and testing," *J. Sound Vib.*, vol. 459, p. 1148650, 2019, doi: 10.1016/j.jsv.2019.1148650.

[30] M. Żurawski, B. Chiliński, and R. Zalewski, "A novel method for changing the dynamics of slender elements using sponge particles structures," *Adv. Mech. Test. Eng. Mater.*, vol. 13, p. 4847, 2020, doi: 10.3390/ma13214874.

[31] R. Espíndola *et al.*, "The double pendulum of variable mass: Numerical study for different cases," *J. Phys.-Conf. Ser.*, vol. 1221, p. 012049, 2019, doi: 10.1088/1742-6596/1221/1/012049.

[32] R. Kwiatkowski, T. Hoffmann, and A. Kołodziej, "Dynamics of a double mathematical pendulum with variable mass in dimensionless coordinates," *Procedia Eng.*, vol. 177, pp. 439–443, 2017, doi: 10.1016/j.proeng.2017.02.242.

[33] M. Dudziak, R. Kwiatkowski, and A. Kołodziej, "The double pendulum as a variable mass system," in *Int. Conf. Methods & Tools for CAE - concepts and applications*, vol. 254, no. 03003, pp. 267–273, 2017.

[34] R. Kwiatkowski, "Movement of double mathematical pendulum with variable mass," *Mach. Dyn. Res.*, vol. 38, no. 2, pp. 47–58, 2014, doi: 10.1016/j.proeng.2017.02.24.

[35] R. Kamgar, F. Gholami, H. Sanayei, and H. Heidarzadeh, "Modified tuned liquid dampers for seismic protection of buildings considering soil–structure interaction effects," *Iran. J. Sci. Technol.-Trans. Civ. Eng.*, vol. 44, pp. 339–354, 2020, doi: 10.1007/s40996-019-00302-x.

[36] A. Hemmati, O. Oterkus, and M. Khorasanchi, "Vibration suppression of offshore wind turbine foundations using tuned liquid column dampers and tuned mass dampers," *Ocean Eng.*, vol. 172, pp. 286–295, 2019, doi: 10.1016/j.oceaneng.2018.11.055.

[37] M. Tarpø, C. Georgakis, A. Brandt, and R. Brincker, "Experimental determination of structural damping of a full-scale building with and without tuned liquid dampers," *J. Int. Assoc. Struct. Control Monit.*, vol. 28, p. e2676, 2020, doi: 10.1002/stc.2676.

[38] D.-P.N. Kontoni and A.A. Farghaly, "Assessing seismic mitigation schemes of tuned mass dampers for monopile offshore wind turbine including pile–soil–structure interaction," *Asian J. Civ. Eng.*, vol. 25, no. 2, pp. 1773–1799, 2024.

[39] B. Zhu, Y. Wu, C. Sun, and D. Sun, "An improved inerter-pendulum tuned mass damper and its application in monopile offshore wind turbines," *Ocean Eng.*, vol. 298, p. 117172, 2024.

[40] G.B. Colherinhas, M.V.G. de Morais, and F. Petrini, "Global vibration control of offshore wind turbines with a flexible monopile foundation using a pendulum-tuned mass damper: Risk mitigation and performance incrementation," *Ocean Eng.*, vol. 297, p. 117168, 2024.

[41] B. Chilinski, A. Mackojc, R. Zalewski, and K. Mackojc, "Proposal of the 3-DOF model as an approach to modelling offshore lifting dynamics," *Ocean Eng.*, vol. 203, p. 107235, 2020, doi: 10.1016/j.oceaneng.2020.107235.

[42] B. Chilinski, A. Mackojc, and K. Mackojc, "Analytical solution of parametrically induced payload nonlinear pendulation in offshore lifting," *Ocean Eng.*, vol. 259, p. 111835, 2022, doi: 10.1016/j.oceaneng.2022.111835.

[43] R. Kwiatkowski, "Dynamic analysis of double pendulum with variable mass and initial velocities," *Procedia Eng.*, vol. 136, pp. 175–180, 2016.

[44] R. Kwiatkowski, "The concept of vibration damping of the variable mass assembly," *MATEC Web Conf.*, vol. 254, p. 03003, 2019.

[45] C.C. Cossette, J.R. Forbes, and D. Saussie, "Lagrangian derivation of variable-mass equations of motion using an arbitrary attitude parameterization," *J. Astronaut. Sci.*, vol. 67, no. 4, pp. 1206–1219, 2020.

[46] M. Zurawski, B. Chilinski, and R. Zalewski, "A novel method for changing the dynamics of slender elements using sponge particles structures," *Materials*, vol. 13, no. 21, p. 4874, 2020.

[47] H. Dresig and F. Holzweissig, *Dynamics of machinery: theory and applications*. Springer Science & Business Media, 2010.